Available online at www.sciencedirect.com
SCIENCE DIRECT®
Solid State Ionics 160 (2003) 227–233
SOLID STATE IONICS
www.elsevier.com/locate/ssi

Surface modification of $LiMn_2O_4$ thin films at elevated temperature

Dong Shu[a,*], Gopu Kumar[a], Kwang-Bum Kim[a], Kwang Sun Ryu[b], Soon Ho Chang[b]

[a] Department of Metallurgical Engineering, Yonsei University, 134 Shinchon-dong, Seodaemun-gu, Seoul 120-749, Korea
[b] Power Source Technology Team, Electronics and Telecommunications Research Institute (ETRI), Daejon 305-350, Korea

Received 30 October 2002; received in revised form 2 May 2003; accepted 9 May 2003

Abstract

In order to improve the cycle stability of spinel $LiMn_2O_4$ electrode at elevated temperature, the $LiCoO_2$-coated and Co-doped $LiMn_2O_4$ film were prepared by an electrostatic spray deposition (ESD) technique. $LiCoO_2$-coated $LiMn_2O_4$ film shows excellent cycling stability at 55 °C compared to pristine and Co-doped $LiMn_2O_4$ films. The samples were studied by X-ray diffraction, scanning electron microscopy, Auger electron spectroscopy, cyclic voltammetry and electrochemical impedance spectroscopy. The excellent performance of $LiCoO_2$-coated $LiMn_2O_4$ film can be explained by suppression of Mn dissolution. On the other hand, the $LiCoO_2$-layer on the $LiMn_2O_4$ surface allows a homogenous Li^+ insertion/extraction during electrochemical cycles and improves its structure stability.

Keywords: Lithium ion battery; $LiMn_2O_4$; Surface modification; Mn dissolution

1. Introduction

Spinel $LiMn_2O_4$ is of great interest for use in lithium ion battery due to its high voltage, low cost and low toxicity. Unfortunately, fast capacity fading at elevated temperature limits its application in commercial cells. The major factors responsible for the capacity fading at the elevated temperature are ascribed as follows: (i) Jahn-Teller distortion caused by presence of Mn^{3+} ions [1]; (ii) Mn dissolution induced by HF acid [2–4]; (iii) the transformation of the unstable two-phase structure to a more stable one-phase structure [5,6]. All the above-proposed factors are mainly associated with the morphology and crystal structure. Therefore, many studies have been reported in these directions. In order to improve the performance of $LiMn_2O_4$ related with surface morphology, many research works have been performed including directly preparing spinel with small surface area [7] and also by coating spinel with $Li_2O-B_2O_3$ [8]. On the other hand, many efforts have been devoted to stabilize its structure by partial substitution of other transition metals into Mn sites [9,10]. However, all these attempts were effective to a certain extent for overcoming the capacity fading at elevated temperature. Recently, significant improvement on the performance of $LiMn_2O_4$ cathode material at elevated temperature has been achieved by sol–gel coating on its particle surface with $LiCoO_2$ [11,12], these attempts have opened up new avenues.

* Corresponding author. Present address: Chemistry Department, Zhaoqing University, Zhaoqing, Guangdong Province, 526061, China. Tel.: +86-758-271-645-2.; fax: +86-758-271-658-6.
E-mail address: shudong66@hotmail.com (D. Shu).

0167-2738/03/$ - see front matter © 2003 Elsevier B.V. All rights reserved.
doi:10.1016/S0167-2738(03)00190-5

Thus, the progress in the microelectronics industry has reduced the current and power requirements of electronic device to an extremely low level, this has made possible the use of thin-film rechargeable microbatteries as a power sources for these devices [13]. Hence, the thin film electrodes show great commercial potential. Further, the thin film electrode has simple geometric form without additives such as a polymer binder and conducting materials and therefore makes the theoretical analysis of their electrochemical performance easier.

In this study, we report the results of a new approach to improve the cycle stability of the $LiMn_2O_4$ electrostatic spray deposition (ESD) thin film electrode at elevated temperature by means of coating of $LiCoO_2$ onto its surface. $LiCoO_2$-coated $LiMn_2O_4$ film shows excellent cycle stability at elevated temperature compared to pristine and Co-doped $LiMn_2O_4$ film. The suppression of Mn dissolution and the improvement of its structure stability can explain the excellent performance of $LiCoO_2$-coated $LiMn_2O_4$ film.

2. Experimental

$LiCoO_2$-coated $LiMn_2O_4$ films were prepared by ESD technique and its working principles have been described in the literature [14–16]. The precursor solution consisted of 25 mM $LiNO_3$ + 50 mM $Mn(NO_3)_2$ in EtOH for $LiMn_2O_4$ layer and 25 mM $LiNO_3$ + 25 mM $Co(NO_3)_3$ for $LiCoO_2$ layer was pumped at 2 ml h^{-1} through a stainless steel nozzle respectively, a distance of 3 cm was kept and a voltage of 10 kV was applied between the nozzle and substrate, all ESD films were deposited on Pt foils. The substrate temperature was maintained at 400 °C during the deposition and then the deposited film was annealed further for 1 h at 600 °C in an air oven. Stoichiometric mixtures of $LiNO_3$, $Co(NO_3)_3$ and $Mn(NO_3)_2$ in EtOH were used for preparation of Co-doped $LiMn_2O_4$. The concentration of Co in both $LiCoO_2$-coated and Co-doped $LiMn_2O_4$ was controlled in 6%.

Scanning electron microscope (SEM, HITACHI S2700) was used for evaluating the surface morphology. The crystal structure of ESD films were characterized by X-ray diffraction (XRD) patterns using Cu Kα radiation in a Rigaku diffractometer.

All electrochemical measurements were carried out using three-electrode cells assembled under argon atmosphere in a glove box. The studies were carried out with the ESD film as the working electrode in nonaqueous electrolyte (1 M $LiPF_6$ + EC + DMC) using lithium foil as reference and counter electrodes. Electrochemical impedance spectroscopy (EIS) measurements were performed using a Solartron 1287 electrochemical interface and 1260 impedance/gain-phase analyzer driven by the Zplot software in the frequency range 10^{-2}–10^5 Hz.

3. Results and discussion

The XRD patterns of $LiMn_2O_4$ thin film obtained by using ESD technique on a Pt foil substrate are presented in Fig. 1. In order to minimize interference from the diffraction peaks of the substrate, near grazing angle scans, were made in which the angle of the incident radiation with respect to the plane of the substrate was fixed at 5° while the detector with a parallel-beam thin-film attachment placed in front of it was moved through 2θ angle. It can be seen clearly that all the hkl peaks could be indexed to the spinel structure of $LiMn_2O_4$ representing the space group, Fd3m. The two peaks of the substrate due to Pt are also marked in Fig. 1. Thus, we can assign the position of Li and Mn ions to the 8a tetrahedral and 16d octahedral sites, respectively [17]. However, due

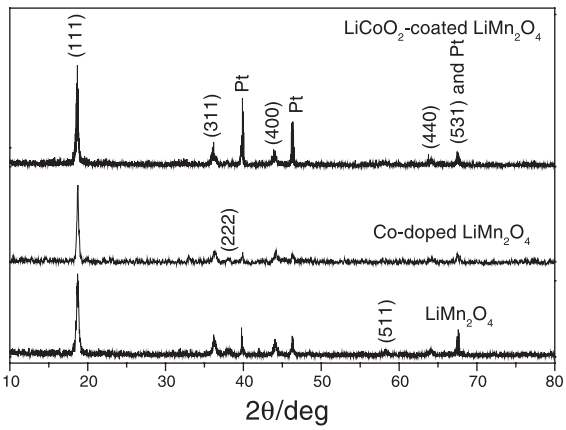

Fig. 1. XRD spectra of $LiMn_2O_4$ film prepared onto Pt substrate by ESD.

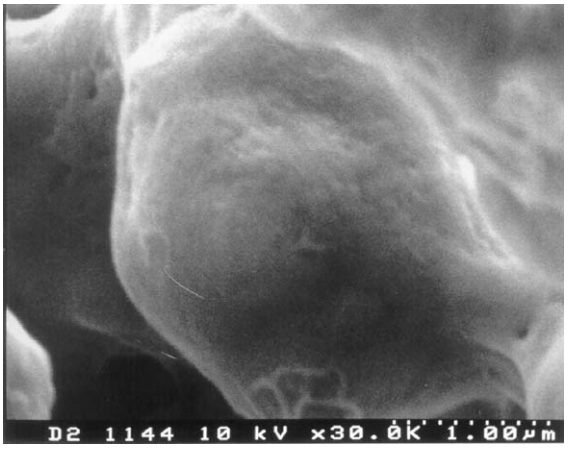

Fig. 2. A SEM image of $LiMn_2O_4$ film by ESD.

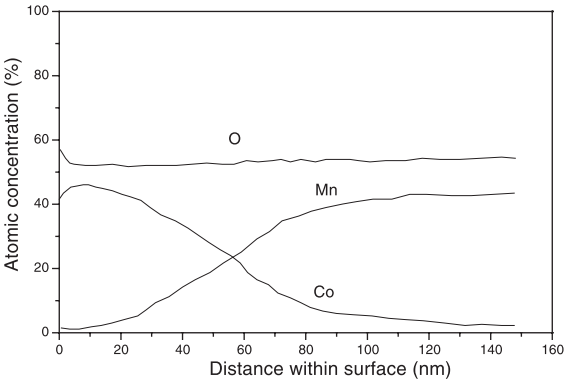

Fig. 4. The concentration profiles of a $LiCoO_2$-coated $LiMn_2O_4$ thin film by AES analysis. The AES analysis was performed with the accelerating voltage of 10 kV.

to almost similar diffraction pattern between $LiMn_2O_4$ and $LiCoO_2$ [12], no extra diffraction peak was detected in $LiCoO_2$-coated and Co-doped $LiMn_2O_4$.

The surface morphology of pristine and $LiCoO_2$-coated $LiMn_2O_4$ film observed by scanning electron microscopy is shown in Figs. 2 and 3, respectively. The surface morphology of pristine $LiMn_2O_4$ is smooth (Fig. 2) but it becomes coarse after a layer of $LiCoO_2$ is coated on the surface of the $LiMn_2O_4$ (Fig. 3). In order to identify the spatial distribution of Co within the surface of $LiMn_2O_4$ thin film, the element concentration profiles were obtained by Auger electron spectroscopy (AES) and shown in Fig. 4. It can be seen that the Co atoms are only distributed on the surface of film. The decrease of the Co content accompanies simultaneously the increase of Mn content toward the bulk of film indicating that $LiCoO_2$ is coated on the $LiMn_2O_4$ surface.

Fig. 5 shows the cyclic voltammogram (CV) of $LiMn_2O_4$ ESD film at room temperature, the pair of oxidation and reduction peaks appear around 4.0 and 4.15 V which is in agreement with the results reported by several researchers [18,19]. The two pairs of redox peaks indicate that spinel $LiMn_2O_4$ experiences a two-

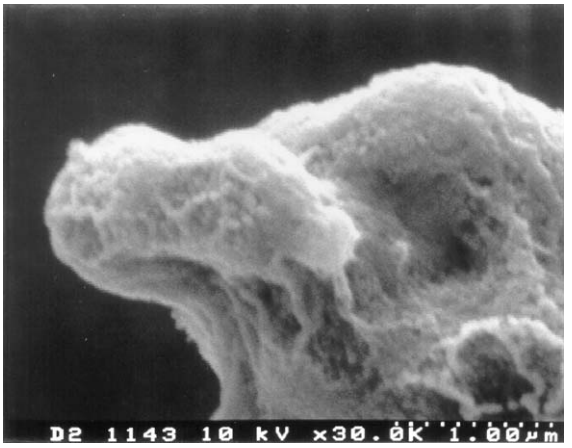

Fig. 3. A SEM image of $LiCoO_2$-coated $LiMn_2O_4$ film by ESD.

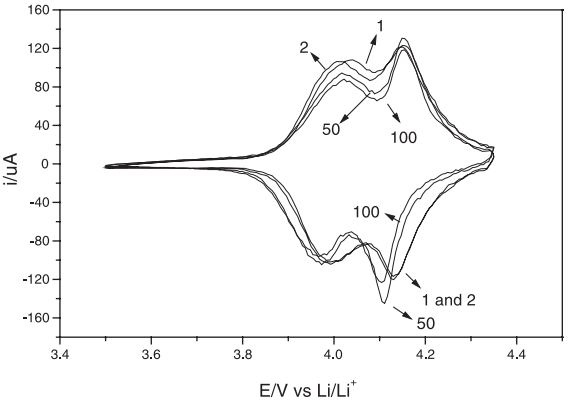

Fig. 5. Cyclic voltammogram of a $LiMn_2O_4$ ESD film at room temperature (scan rate 0.2 mV s^{-1}, electrolyte 1 M $LiPF_6$ + EC + DMC).

step reaction during extraction/insertion of Li^+ ions in the 4 V region, and the electrochemistry clearly suggests the existence of an intermediate phase between initial $LiMn_2O_4$ and λ-MnO_2 [20]. Symmetric current peaks observed in Fig. 5 imply good kinetic response due to short diffusion distance of Li^+ ions in ESD film. The result also shows only 12% capacity loss after 100 cycles and demonstrates the good reversible cycling behavior of $LiMn_2O_4$ ESD film at room temperature. However, fast capacity fading of $LiMn_2O_4$ ESD film is observed in Fig. 6 when the CV experiment was performed at 55 °C. The fast capacity fading of $LiMn_2O_4$ is a main obstacle for its commercial application. It is well known that the reversibility of spinel $LiMn_2O_4$ can be improved by doping of various metal ions such as Li^+, Co^{2+}, Ni^{2+}, Zn^{2+}, Mg^{2+}, Ga^{2+}, Al^{3+} and Cr^{3+}. These doping ions substitute for Mn^{3+}occupying the 16d octahedral sites in the spinel phase. As seen from CV of Co-doped $LiMn_2O_4$ at 55 °C (Fig. 7), the introduction of Co^{3+} into 16d octahedral sites in the spinel phase improves the reversibility of $LiMn_2O_4$. However, it is seen from Fig. 9, that the capacity fading of Co-doped $LiMn_2O_4$ after 50 cycles remains at 26%, so the improvement of reversibility by doping Co is limited to some extent at 55 °C. Fig. 8 shows the CV of $LiCoO_2$-coated $LiMn_2O_4$ at 55 °C and indeed the $LiCoO_2$-coated $LiMn_2O_4$ shows excellent reversibility, the capacity fading after 50 cycles is seen to be only 11% (Fig. 9). Further, it is observed in Figs. 5–8 that broad redox peaks (Figs. 5 and 7) can be related with good reversibility.

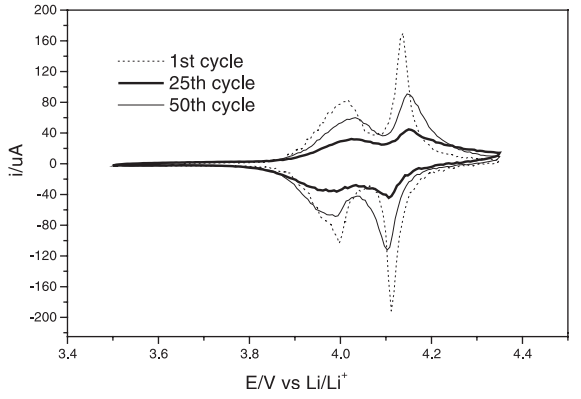

Fig. 6. Cyclic voltammogram of a $LiMn_2O_4$ ESD film at 55 °C (scan rate 0.2 mV s^{-1}, electrolyte 1 M $LiPF_6$ + EC + DMC).

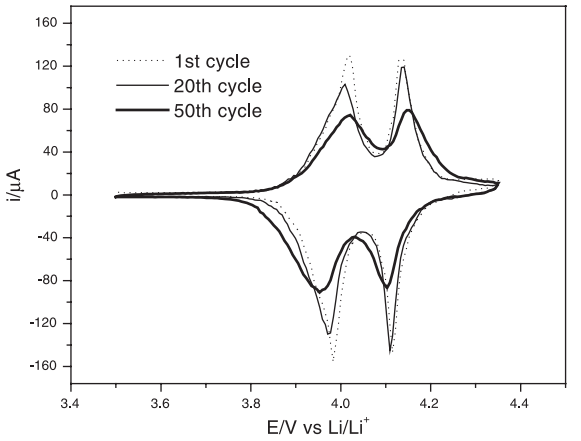

Fig. 7. Cyclic voltammogram of a Co-doped $LiMn_2O_4$ (6%) ESD film at 55 °C (scan rate 0.2 mV s^{-1}, electrolyte 1 M $LiPF_6$ + EC + DMC).

It is well known the main factors contributing to the capacity fading of spinel $LiMn_2O_4$ electrode are ascribed as follows:

(1) *Jahn-Teller distortion*: Jahn-Teller distortion takes place when Li^+ ions insert into $LiMn_2O_4$ in 3 V region, it results a phase transformation from a cubic to tetragonal symmetry. However in the present case, the CV experiments were performed in 4 V region (3.5–4.4 V), so Jahn-Teller distortion could be ruled out as a major contributor to capacity fading.

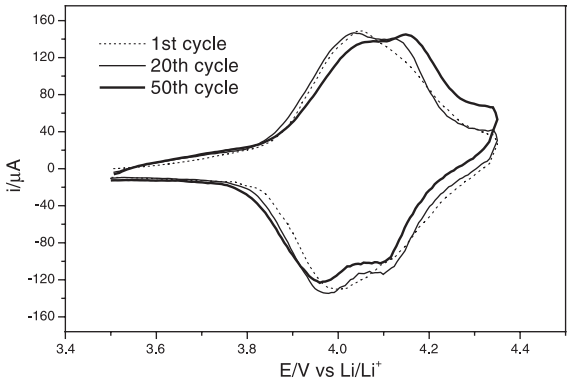

Fig. 8. Cyclic voltammogram of a $LiCoO_2$-coated $LiMn_2O_4$ (6%) ESD film at 55 °C (scan rate 0.2 mV s^{-1}, electrolyte 1 M $LiPF_6$ + EC + DMC).

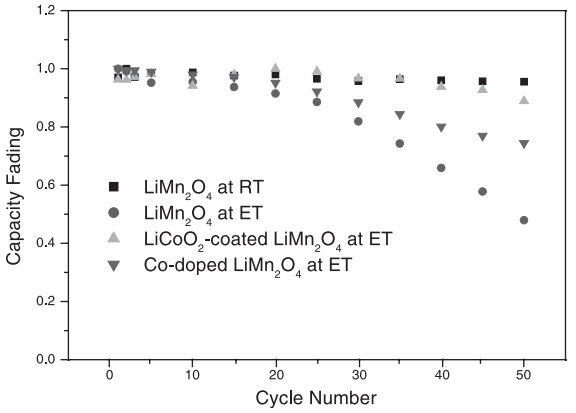

Fig. 9. Capacity fading as a function of cycle number of $LiMn_2O_4$ ESD film (scan rate 0.2 mV s^{-1}, electrolyte 1 M $LiPF_6$ + EC + DMC).

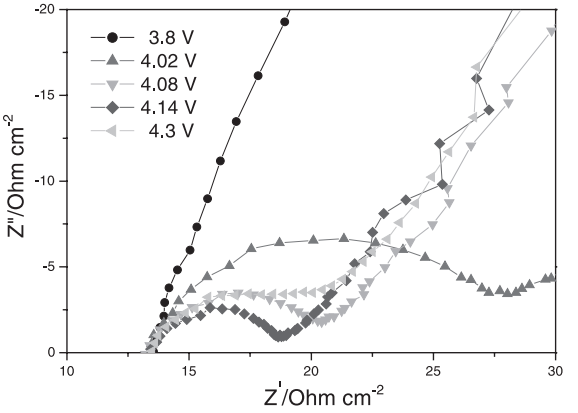

Fig. 10. Nyquist plots measured from the $LiMn_2O_4$ ESD film before CV cycle at the different potential as indicated.

(2) *Mn dissolution*: Mn dissolution is induced by HF acid generated by temperature-enhanced electrolyte decomposition. Excellent reversibility of $LiCoO_2$-coated $LiMn_2O_4$ ESD film implies that the Mn dissolution is blocked by a layer of $LiCoO_2$ on $LiMn_2O_4$ film surface. It is well known that $LiCoO_2$ exhibits excellent performance at elevated temperature, so the layer of $LiCoO_2$ on the surface of $LiMn_2O_4$ prevents direct contact between the spinel and the electrolyte thereby suppressing the Mn dissolution which is responsible for the capacity fading.

(3) *Structure instability*: Xia et al. [5,7] pointed out that the transformation of an unstable two-phase to a more stable one-phase structure takes place during the extraction/insertion of Li^+ ions and is accompanied by the loss of MnO. The structural instability results in the capacity fading of the spinel $LiMn_2O_4$. The two pairs of redox peaks in Figs. 5–8 indicate phase change during the extraction/insertion of Li^+ ions. At elevated temperature, the sharp redox peaks in the CVs of pristine and Co-doped $LiMn_2O_4$ suggest that phase change is focused on a narrow potential region, and the sudden phase change results in the poor reversibility due to its structural instability. The CVs of $LiMn_2O_4$ film at room temperature and $LiCoO_2$-coated $LiMn_2O_4$ at 55 °C reveal that the phase change take place in a large potential region, so this process is relatively smooth and the structure is more stable thereby exhibiting excellent reversibility. Further, at elevated temperature, a layer of $LiCoO_2$ on $LiMn_2O_4$ surface allow a homogenous Li^+ insertion/extraction in the entire 4 V intercalated region, thereby stabilizing the structure of spinel phase and improving the reversibility of $LiCoO_2$-coated $LiMn_2O_4$. Recently, Hwang et al. [21] confirmed by XRD that the structure stability of spinel $LiMn_2O_4$ improved after $LiMn_2O_4$ core was surrounded by $LiCo_xMn_{2-x}O_4$ shell material.

Electrochemical impedance spectroscopy is one of the most powerful techniques for investigating the nature of an electrode during an electrochemical

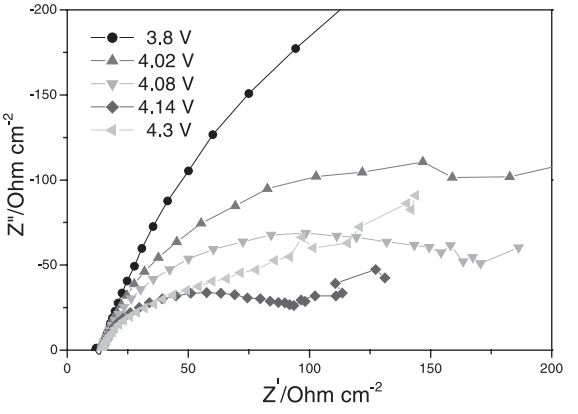

Fig. 11. Nyquist plots measured from the $LiMn_2O_4$ ESD film after 40th CV cycle at the different potential as indicated.

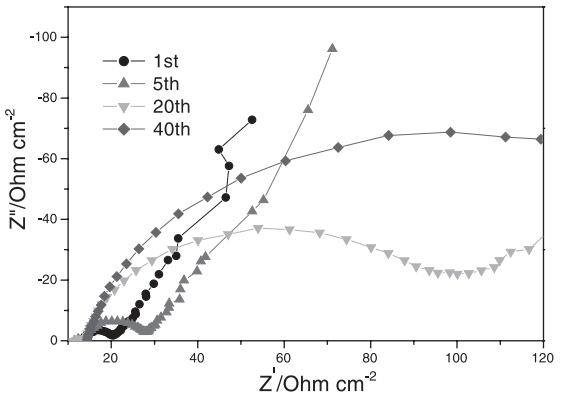

Fig. 12. Nyquist plots measured from $LiMn_2O_4$ ESD film at 4.08 V at the different cycle number as indicated.

process. Structural change of $LiMn_2O_4$ ESD film should therefore affect the impedance behavior. Hence, the EIS measurements of $LiMn_2O_4$ ESD film were performed in different potentials and cycles.

The Nyquist plots of fresh $LiMn_2O_4$ ESD film are shown in Fig. 10, the measurements were performed at 55 °C. The EIS profiles at certain potential consist of a semicycle and a straight line. The simicycle is related to charge transfer resistance (R_{CT}) and double layer capacitance. The straight line ascribes to Warburg impedance due to diffusion process. Fig. 10 shows that a minimum value of R_{CT} appears at 4.14 V with the increase of potential from 3.8 to 4.3 V and is in accordance with the observation of several other researches [22–24].

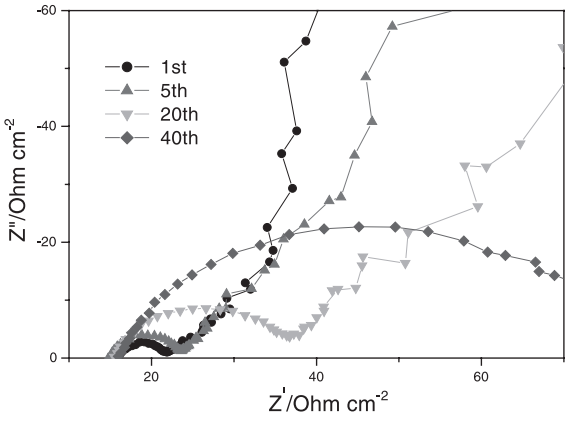

Fig. 13. Nyquist plots measured from $LiCoO_2$-coated $LiMn_2O_4$ ESD film at 4.08 V at the different cycle number as indicated.

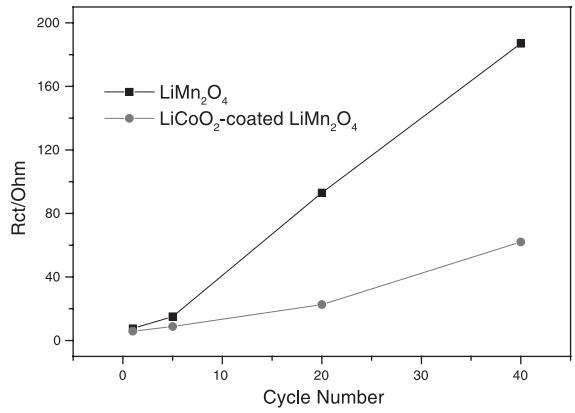

Fig. 14. R_{CT} vs. cycle number deduced from EIS data of pristine and $LiCoO_2$-coated $LiMn_2O_4$ ESD film at 4.08 V.

Fig. 11 show the EIS profiles of $LiMn_2O_4$ ESD film after 40 cycles. Similar tendency could be observed but R_{CT} becomes larger. The increase in R_{CT} value could be ascribed to the structural changes. The EIS measurements were also carried out using $LiCoO_2$-coated $LiMn_2O_4$ (6%) ESD film. In order to compare the difference between the pristine and $LiCoO_2$-coated $LiMn_2O_4$ film, a peak potential of 4.08 V was selected, the developments of impedance vs. cycle number are shown in Figs. 12 and 13. The R_{CT} increases with the increase of cycle number in both the electrodes. Fig. 14 shows the R_{CT} change vs. cycle number from EIS data, the R_{CT} values are similar in both fresh electrodes, but after 40 cycles, the R_{CT} in pristine $LiMn_2O_4$ electrode is four times more than the R_{CT} in $LiCoO_2$-coated $LiMn_2O_4$. This result suggests that more structural change takes place during the CV cycles in pristine $LiMn_2O_4$ film electrode, therefore the structure stability of $LiMn_2O_4$ film improves after a layer of $LiCoO_2$ is coated on its surface.

4. Conclusion

The surface of $LiMn_2O_4$ film was coated with a layer of $LiCoO_2$ using ESD method. $LiCoO_2$-coated $LiMn_2O_4$ (6%) ESD film showed an excellent reversibility than pristine one at elevated temperature (55 °C). The reason for the improvement at elevated temperature is that the layer of $LiCoO_2$ preserves the

surface of $LiMn_2O_4$ from the electrolyte, which results in the suppression of Mn dissolution. Further, the $LiCoO_2$ layer on the $LiMn_2O_4$ surface allows a homogenous Li^+ insertion/extraction and improves its structure stability during the electrochemical cycling.

Acknowledgements

This work was supported by the Ministry of Information and Communication (MIC) in Korea (2002-S-013).

References

[1] R.J. Gummow, A. de Kock, M.M. Thackerey, Solid State Ionics 69 (1994) 59.
[2] M.M. Thackerey, J. Am Ceram. Soc. 82 (1999) 3347.
[3] A. Blyr, C. Sigala, G.G. Amatucci, D. Guyomard, Y. Chabre, J.M. Tarascon, J. Electrochem. Soc. 145 (1998) 194.
[4] X. Sun, H.S. Lee, X.Q. Yang, J. McBreen, Electrochem. Solid-State Lett. 4 (2001) A184.
[5] Y. Xia, Y. Zhou, M. Yoshio, J. Electrochem. Soc. 144 (1997) 2593.
[6] S.J. Wen, T.J. Richardson, L. Ma, K.A. Striebel, P.N. Ross Jr., E.J. Cairins, J. Electrochem. Soc. 143 (1996) L136.
[7] Y. Xia, N. Kumada, N. Yoshio, J. Power Sources 90 (2000) 135–138.
[8] G.G. Amatucci, A. Blyr, C. Siagala, P. Alfonse, J.M. Tarasconm, Solid State Ionics 104 (1997) 13.
[9] A. Antonini, C. Bellitto, M. Pasquali, G. Pistoia, J. Electrochem. Soc. 145 (1998) 2726.
[10] Y. Xia, Y. Hideshima, N. Kumada, M. Nagano, M. Yoshio, J. Power Sources 74 (1998) 24.
[11] J. Cho, G.B. Kim, H.S. Lim, et al., Electrochem. Solid-State Lett. 2 (12) (1999) 607–609.
[12] S.-C. Park, Y.-S. Han, Y.-S. Kang, et al., J. Electrochem. Soc. 148 (7) (2001) A680–A686.
[13] M. Mohamedi, D. Takahashi, T. Itoh, M. Umeda, I. Uchida, J. Electrochem. Soc. 149 (1) (2002) A19–A25.
[14] C.H. Chen, E.M. Kelder, M.J.G. Jak, J. Schoonman, Solid State Ionics 86–88 (1996) 1301–1306.
[15] C. Chen, E.M. Kelder, P.J.J.M. Van der Put, J. Schoonman, J. Mater. Chem. 6 (5) (1996) 765–771.
[16] A.A. van Zomeren, E.M. Kelder, J.C.M. Marunissen, J. Schoonman, J. Aerosol Sci. 25 (1994) 1229.
[17] D. Zhang, B.N. Popov, R.E. White, J. Power Source 76 (1998) 81.
[18] M. Nishizawa, T. Uchiyama, T. Itoh, T. Abe, I. Uchida, Langmuir 15 (1999) 4949–4951.
[19] K.Y. Chung, K.-B. Kim, J. Electrochem. Soc. 149 (1) (2002) A79–A85.
[20] X. Sun, X.Q. Yang, M. Balasubramanian, J. McBreen, Y. Xia, T. Sakai, J. Electrochem. Soc. 149 (7) (2002) A842–A848.
[21] B.J. Hwang, R. Santhanam, C.P Huang, Y.W. Tsai, J.F. Lee, J. Electrochem. Soc. 149 (2002) A694–A698.
[22] D. Aurbach, K. Gamolsky, B. Markovsky, G. Salitra, Y. Gofer, U. Heider, R. Oesten, M. Schmidt, J. Electrochem. Soc. 147 (4) (2000) 1322–1331.
[23] G.X. Wang, D.H. Bradhurst, H.K. Liu, S.X. Dou, Solid State Ionics 120 (1999) 95–101.
[24] D. Shu, K.Y. Chung, W.I. Cho, K.-B. Kim, J. Power Source 114 (2003) 253–263.